Egypt. J. Chem. **Vol. 68**, No. 5 pp. 263 - 269 (2025)

Egyptian Journal of Chemistry

http://ejchem.journals.ekb.eg/

Tuning Electrospinning Conditions to Tailor the Diameter and Morphology of Polycaprolactone Nanofibers

Reem Fathy[1], A.M. Abdelghany[2], W.I. Mortada[3], E Abdel-Latif[1]

[1]Department of Chemistry, Faculty of Science, Mansoura University, 35516, Mansoura, Egypt
[2]Spectroscopy Department, Physics Research Institute, National Research Centre, 33 ElBehouth St., Dokki, 12311, Giza, Egypt
[3]Clinical Chemistry Laboratory, Urology and Nephrology Center, Mansoura University, Mansoura 35516, Egypt

Abstract

The diameter and morphology of polycaprolactone (PCL) nanofibers were optimized by varying electrospinning conditions including applied voltage, concentration of PCL solution, feed rate, and spinneret-collector distance, to obtain smooth and bead-free nanofibers. Scanning electron microscope and Fourier-transform infrared spectroscopy were used to characterize the obtained nanofibers. The results revealed that smooth, bead-free PCL nanofibers were acquired at an applied voltage of 20 kV, polymer concentration of 10.0 m/v %, feed rate of 0.5 mL h^{-1}, and spinneret-collector distance of 15.0 cm. SEM image show continuos uniform and smooth surface fibrous structure of electrospun PCL fibers with average diameter of 170.87nm. This demonstrated the synergistic effect of optimizing multiple electrospinning parameters on the diameter and morphology of PCL nanofibers.

Keywords: Electrospinning; Polycaprolactone; Nanofiber; Morphology; Diameter

1-Introduction

Recent advances in nanotechnology have enabled the fabrication of functional polymeric nanofibers that show promising utilization in various fields that include water treatment, tissue engineering, biosensing, drug delivery, and more[1–3]. Initial research on tissue regeneration focused on natural polymers like alginate, chitosan, gelatin, silk, and collagen, due to their biocompatibility, biodegradability, and solubility[4]. However, these materials faced challenges like poor mechanical properties, high cost, difficult processability, and limited availability[5,6]. This prompted the creation of artificial biodegradable polymer fibers, which not only provide advantages like flexible, controllable designs, and tailored mechanics, but also eliminate these disadvantages[7]. Various research groups have explored the use of artificial polymers including polycaprolactone (PCL), polyvinyl alcohol, polylactic acid (PLA), and others for diverse applications[6–9]. These synthetic polymers provide more flexibility in tuning mechanical strength, degradation rates, and fabrication processes to meet the demands of different bioengineering applications. To fully realize the potential of creative synthetic polymeric nanofiber systems in environmental remediation, medicine, and other fields, more research is still required[4,10].

Polycaprolactone (PCL) is the best material to prepare nanofibers with a procedure for electrospinning that produces superior biocompatibility[11–13]. PCL is a nontoxic, biodegradable, thermal stable polymer with good biocompatibility[14]. PCL is involved in many applications including wound dressings, bone engineering, artificial blood vessels, membrane and food packaging systems[13,15,16]. The technique of electrospinning allows for the preparation of fibers from a variety of materials at the micro-to nano scale. When a liquid polymer is exposed to a high voltage, a continuous jet strand is ejected from the spinneret and moves in the direction of a grounded collector. The supplied electric field overcomes the polymer droplet's surface tension. After that, the droplet elongates to create a "Taylor cone," which is then extruded to create a fiber jet. As the fiber jets pass through the environment, the solvent in them evaporates, depositing solid polymer fibers as a nonwoven web on the metal collector[17]. As has been extensively documented, several processing factors, such as voltage, flow rate, type of collector, and distance of collector, have a major effect on the fiber morphology during the electrospinning process. In addition, there are solution factors that also influence the size and morphology of nanofiber such as concentration, viscosity,

*Corresponding author: w.mortada@mans.edu.eg.; (Dr. Wael Mortada).
Received date 22 August 2024; revised date 25 September 2024; accepted date 30 September 2024
DOI: 10.21608/EJCHEM.2019.6778.1566

type of polymer, and molecular weight of polymer, as well as ambient conditions (humidity and room temperature)[18–23]. The applied voltage and concentration of the polymer solution are the most crucial factors for regulating the nanofibers' morphology, which is necessary for the jet formation to occur. When the applied voltage is low, the surface tension of the polymer solution is not sufficiently overcome by the Coulombic forces, causing droplets or beads to form rather than smooth fibers[24]. As the voltage is raised, the balance of the viscoelastic and superficial tension creates a charged jet and small fiber diameters. Higher applied voltages cause the jet to break and larger diameters to be produced because the Coulombic forces outweigh the viscoelastic forces[24]. The concentration affects the viscosity of the solution so when the concentration is very low the electrospray is produced instead of smooth fiber. By increasing the concentration until reach the adjusted concentration, the fiber without beads will be prepared but at a very high concentration, for the fiber with micro diameter, not nano[4].

The presented work aimed to modify the different electrospinning parameters such as applied voltage, polymer solution concentration, feed rate, and spinneret-collector distance to generate homogenous PCL nanofibers for scaffolds for tissue engineering and water treatment are provided by the findings.

2. Experimental (Materials and Methods)

2.1. Materials

PCL (average molecular weight of 80000 g/mol) was obtained from Sigma-Aldrich Co., USA. Dimethyl formamide (DMF, 99.9% purity) and chloroform ($CHCl_3$, 99.8% purity) were used as solvents in this work are all analytical grade.

2.2. Preparation of PCL nanofibers

PCL solution (10 m/v%) was prepared by stirring an appropriate amount of PCL in chloroform: DMF mixture (8:2) for 4 h. Chloroform was good solvent for PCL but small amount of DMF was added to improve the conductivity of the solution because surface tension cannot be overcome by electrostatic force if the solution is completely insulating or if the applied voltage is insufficient. On the other hand, a polymer solution's spinnability improves with increasing conductivity. As a result, it was concluded that using mix of chloroform and DMF as a solvent made electrospin fibers extremely thin, similar result with another solvent was reported[25]. The obtained solution was loaded into a plastic syringe. The technique of electrospinning (electrospinning-Nanon-01A) was used to create electrospun nanofibers. Sampling was achieved at a temperature of 25±2°C and a relative humidity of 50%±1% in the laboratory. To enable the evaporation of any remaining solvent, all samples were allowed to dry for a full night prior to analysis. To obtain electrospun PCL fibrous samples at 15, 20, and 25 kV, the voltage that was applied was regarded as a variable, while the other parameters remained unchanged as indicated in Table 1. Likewise, the Spinneret-Collector distance was used as a variable for preparing PCL fibers at 12, 13, and 15 cm with constant other parameters as illustrated in Table 1**.** Various concentrations (7, 10, and 14 m/v%) were prepared to study the effect of solution concentration with keeping the remaining other parameters constant. In addition to the feed rate (0.2, 0.5, and 1.0 $ml.h^{-1}$) were taken as variable parameters while maintaining other parameters constant as shown in Table 1.

2.3. Characterization

2.3.1 Scanning electron microscope

Field emission Quanta 250 FEG Scanning Electron Microscope (SEM) (FEI Company, Netherlands) was utilized to study the morphology of the prepared fibers.

2.3.2 Fourier transform infrared (FTIR)

It was performed on i10 Nicolet FTIR (Thermo Fisher, MA, USA). The scans were performed from 4000 - 400 cm^{-1} to elucidate the chemical composition.

Table 1: Preparation of nanofiber samples with different parameters

Variables	Voltage (kV)	S-C Distance (cm)	Feed Rate (ml/h)	Conc of PCL solution (m/v%)	Diameter of fiber (nm)
Concentration	20	15	0.5	7.0	-
	20	15	0.5	10	170.87
	20	15	0.5	14	282.92
Applied	15	15	0.5	10	241.30
Voltage	20	15	0.5	10	237.83
	25	15	0.5	10	251.74
Feed Rate	20	15	0.2	10	302.5
	20	15	0.5	10	225.56
	20	15	1.0	10	454.73
S-C Distance	20	12	0.5	10	336.48
	20	15	0.5	10	351.36
	20	15	0.5	10	351.36

3. Results and discussion

3.1. FTIR analysis

Fig.1 shows FTIR spectra data of PCL in the wave number range of 4000-500 cm^{-1}. Asymmetric and symmetric CH_2 stretching around 2935 cm^{-1} and 2848 cm^{-1} respectively can be observed[26,27]. A sharp signal at 1720 cm^{-1} was related to the carbonyl stretching group (C=O). The peak at 1286 cm^{-1} represents the C-O and C-C groups. Asymmetric COC stretching and OC–O stretching was appeared around 1238 cm^{-1} and 1163 cm^{-1}, respectively.

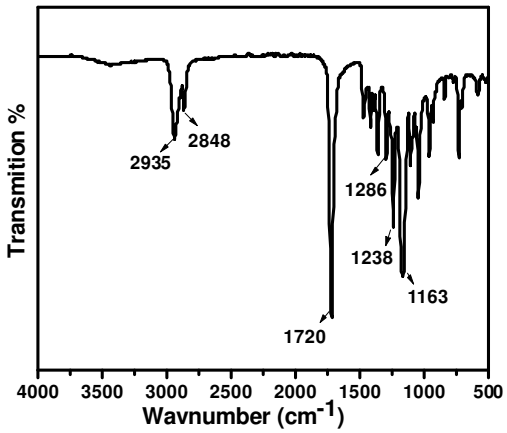

Figure 1: FTIR of PCL nanofiber

3.2. SEM micrographs

SEM micrographs in **Fig.2** were obtained with voltages of 15, 20, and 25 kV. It was observed at a voltage ≤15 kV, that droplet and beads formed on the fiber's membrane. The applied voltage has a direct impact on the quantity of charges carried by the jet, the strength of its interactions with the external electric field, and the degree of electrostatic repulsion between the charged species. Higher voltages typically encourage a decrease in fiber thickness, but they can also cause more fluid to be ejected, which causes fibers to form with thicker diameters [28]. From **Fig.2,** we can see that increasing the voltage to 20 kV decreases in mean fiber diameter. This might have occurred because the stream performed more charge at higher applied voltages, enhancing the Coulomb repulsive and electrostatic forces. This, in turn, may have increased the tensile force on the jet, causing the fiber diameter to decrease. However, it was observed the mean fiber diameter rose when the voltage increased from 20 to 25 kV (from 237.83 to 251.74 nm) as shown in (**Fig.2, Table1**). The reason for this could be that at higher voltages 25 kV, more polymer liquid is induced to be ejected. Furthermore, we can deduce from the observed data that, at the applied voltage of 20kV, uniform smooth fibers without beads were produced. Concentration was less than or equal to 7 m/v%, it was observed that electrospraying formed instead of nanofibers poor fiber uniformity, as shown in **Fig.3**. When the concentration of the polymer solution exceeded 14 m/v%, the syringe needle would frequently block because of the viscosity of the solution and form a fiber with a high diameter. Thus, the optimum concentration is between 7 and 14 m/v% PCL. It was observed from **Fig.3, 4** at 10 m/v% the fibers without beads were formed with thin diameter 170.87nm. A higher concentration of the polymeric solution causes the solution to become more viscous and increases the entanglements in the polymer chains, which increases the size of the fibers [29], its diameter was282.92nm **Table1**. Additionally, we can deduce from the observed data that uniform, bead-free fibers were achieved at 10 m/v% PCL solution. As shown in **Fig.5**, the SEM images were acquired at feed rates of 0.2, 0.5, and 1.0 $ml.h^{-1}$. Through the process, it was observed that under 0.5 $ml.h^{-1}$, the feed rate was very low to see the Taylor cone creation and form electrospray instead of fiber or form fiber with beads, and the fibers' diameter reduced from 302.50 to 225.56 nm as the flow rate increased. However, at a high feed rate >1.0 $ml.h^{-1}$ the diameter of the fibers increases as shown in **Table1** and fibers contain a few beads because with high feed rate does not give the solution sufficient time to charge. Thus, the optimum feed rates tested were within the range of 0.5 to 1.0 $ml.h^{-1}$. A statistically significant reduction in the average diameter as the feed rate is raised has not been documented in many studies. However, some researchers found that an increase in feed rate caused an increase in the volume that was ejected, which in turn caused the fiber diameter to increase[30,31]. Furthermore, we can conclude from the observed data that a uniform bead-free fiber flow rate of 0.5 $ml.h^{-1}$ was achieved.

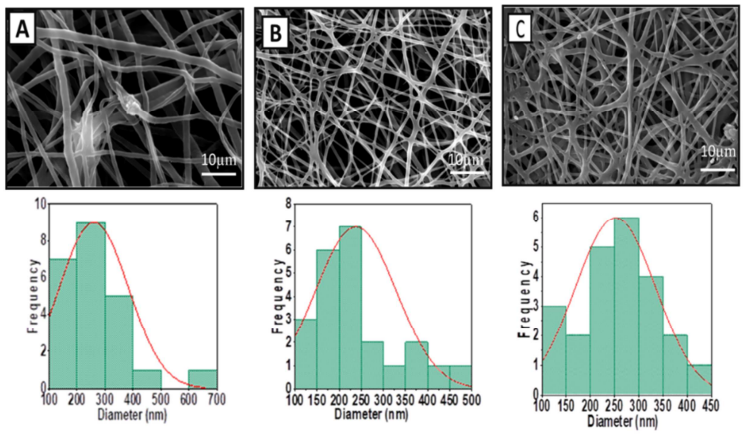

Figure 2: SEM images acquired at voltages applied of (a) 15 kV (b) 20 kV (c) 25 kV as well as their distribution charts, respectively.

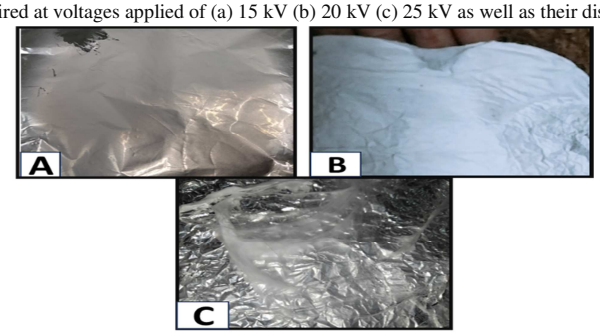

Figure 3: Camera picture of fibers at concentrations of the polymer solution of (a) 7 m/v%, (b) 10 m/v%, and (c) 14 m/v%.

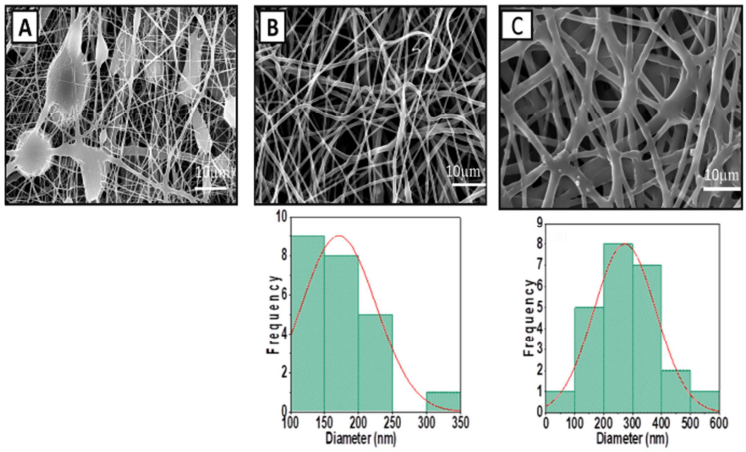

Figure 4: SEM images acquired at concentrations of the polymer solution of (a) 7 m/v%, (b) 10 m/v%, and (c) 14 m/v% as well as their distribution charts, respectively.

The SEM images acquired at spinneret-collector distances of 12, 13, and 15 cm were illustrated in **Fig.6**, respectively. The Spinneret-Collector distance of 12 cm shows the presence of a bead formation. The tested spinneret-collector distances at a high distance because a perfect spinneret-collector distances varies depending on the polymer system and ought to ensure that the jets fully extend and solidify, forming solid fibers as a result. It was observed from **Fig.6** that when the spinneret-collector distances increase from 12 to 15 cm, the fiber diameter decreases. It was shown from Table1 at distance 12cm, the fiber with small diameter was formed but with beads. This aligns with research carried out by Matabola *et al.* and Wang *et al.* with various polymer systems[32,33]. Based on the data, we can deduce that consistent fibers without beads were obtained at a Spinneret-Collector distance of 15 cm.

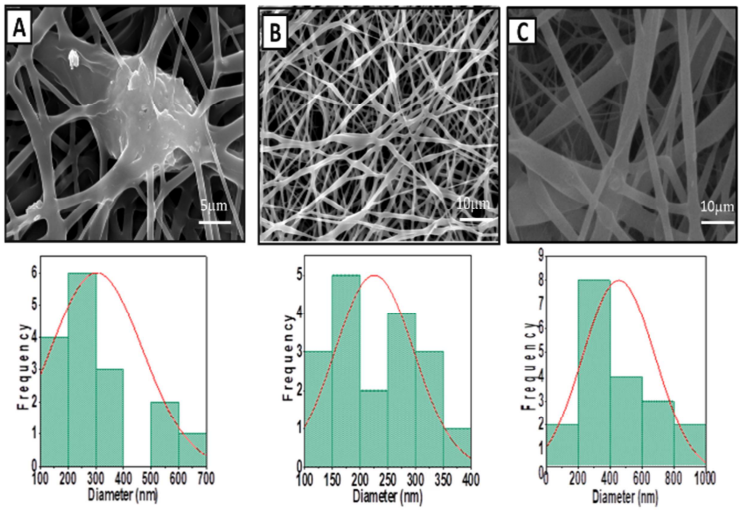

Figure 5: SEM pictures obtained at polymer solution feed rates of (a) 0. 2ml.h^{-1}, (b) 0. 5ml.h^{-1}, and (c) 1.0 ml.h^{-1} as well as their distribution charts, respectively.

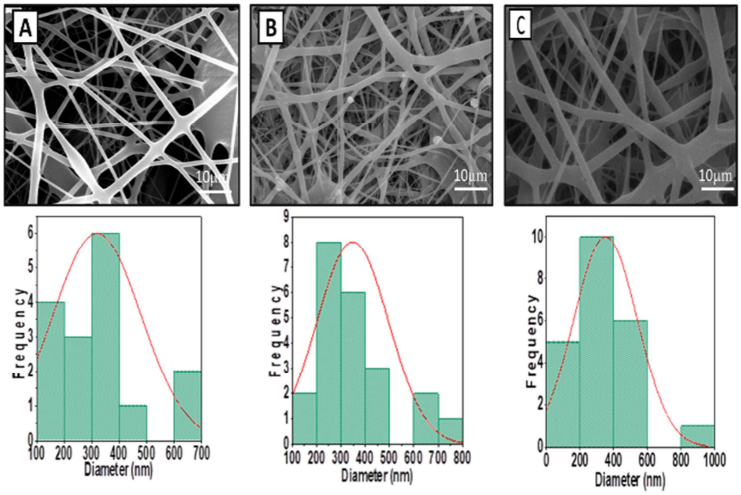

Figure 6: SEM pictures obtained at distance between tip and collector (A) 12cm, (B) 13cm, and (C) 15cm as well as their distribution charts, respectively.

Future research is required to ascertain whether these nanofibers can be used in a variety of applications by examining the relationship between the morphology and mean fiber diameters and mechanical properties. Therefore, to achieve a PCL membrane, mechanical properties must be optimized by adjusting different electrospinning parameters.

4. Conclusion

In conclusion, this study demonstrated that fine-tuning key electrospinning parameters has a significant impact on the size and morphology of electrospun PCL nanofibers. The applied voltage of 20 kV resulted in uniform fibers, while higher voltages caused beading. An optimal polymer concentration of 10 m/v% was established. Lower concentrations yielded non-uniform fibers while higher ones caused clogging. A feed rate of 0.5 ml.h^{-1} produced nanofibers without beads. Furthermore, increasing the spinneret-collector distance reduced fiber diameter. The average diameter of PCL nanofiber is 170.87nm. Ultimately, the synergistic optimization of multiple electrospinning variables is necessary to fabricate bead-free PCL nanofibers with the desired morphology and diameter. In the future, nanofibers will be updated by some additive and will be used for water treatment.

5. Conflict of Interest

The authors declare no conflict of interest

6. References

[1] L. Lou, O. Osemwegie, S.S. Ramkumar, Functional Nanofibers and Their Applications, Ind. Eng. Chem. Res. 59 (2020) 5439–5455. https://doi.org/10.1021/acs.iecr.9b07066.

[2] K. Badgar, N. Abdalla, H. El-Ramady, J. Prokisch, Sustainable Applications of Nanofibers in Agriculture and Water Treatment: A Review, Sustain. 14 (2022) 1–17. https://doi.org/10.3390/su14010464.

[3] V. Tayebi-Khorrami, P. Rahmanian-Devin, M.R. Fadaei, J. Movaffagh, V.R. Askari, Advanced applications of smart electrospun nanofibers in cancer therapy: With insight into material capabilities and electrospinning parameters, Elsevier B.V., 2024. https://doi.org/10.1016/j.ijpx.2024.100265.

[4] Y. Duan, L. Kalluri, M. Satpathy, Y. Duan, Effect of Electrospinning Parameters on the Fiber Diameter and Morphology of PLGA Nanofibers, Dent. Oral Biol. Craniofacial Res. (2021) 1–7. https://doi.org/10.31487/j.dobcr.2021.02.04.

[5] K. Min, S. Kim, S. Kim, Silk protein nanofibers for highly efficient, eco-friendly, optically translucent, and multifunctional air filters, Sci. Rep. 8 (2018) 1–10. https://doi.org/10.1038/s41598-018-27917-w.

[6] Y. Duan, Z. Wang, W. Yan, S. Wang, S. Zhang, J. Jia, Preparation of collagen-coated electrospun nanofibers by remote plasma treatment and their biological properties, J. Biomater. Sci. Polym. Ed. 18 (2007) 1153–1164. https://doi.org/10.1163/156856207781554019.

[7] A. Refate, Y. Mohamed, M. Mohamed, M. Sobhy, K. Samhy, O. Khaled, K. Eidaroos, H. Batikh, E. El-Kashif, S. El-Khatib, S. Mehanny, Influence of electrospinning parameters on biopolymers nanofibers, with emphasis on cellulose & chitosan, Heliyon 9 (2023) e17051. https://doi.org/10.1016/j.heliyon.2023.e17051.

[8] T.C. Mokhena, M.J. Mochane, A. Mtibe, M.J. John, E.R. Sadiku, J.S. Sefadi, Electrospun alginate nanofibers toward various applications: A review, Materials (Basel). 13 (2020) 1–24. https://doi.org/10.3390/ma13040934.

[9] T.M. Dinis, R. Elia, G. Vidal, Q. Dermigny, C. Denoeud, D.L. Kaplan, C. Egles, F. Marin, 3D multi-channel bi-functionalized silk electrospun conduits for peripheral nerve regeneration, J. Mech. Behav. Biomed. Mater. 41 (2015) 43–55. https://doi.org/10.1016/J.JMBBM.2014.09.029.

[10] D.P. Bhattarai, L.E. Aguilar, C.H. Park, C.S. Kim, A review on properties of natural and synthetic based electrospun fibrous materials for bone tissue engineering, Membranes (Basel). 8 (2018). https://doi.org/10.3390/membranes8030062.

[11] N.J. Clerici, A.A. Vencato, R. Helm Júnior, D.J. Daroit, A. Brandelli, Electrospun Poly-ε-Caprolactone Nanofibers Incorporating Keratin Hydrolysates as Innovative Antioxidant Scaffolds, Pharmaceuticals 17 (2024) 1–16. https://doi.org/10.3390/ph17081016.

[12] V. Rahimkhoei, M. Padervand, M. Hedayat, F. Seidi, E.A. Dawi, A. Akbari, Biomedical applications of electrospun polycaprolactone-based carbohydrate polymers: A review, Int. J. Biol. Macromol. 253 (2023) 126642. https://doi.org/10.1016/j.ijbiomac.2023.126642.

[13] G.Ö. Kayan, A. Kayan, Polycaprolactone Composites/Blends and Their Applications Especially in Water Treatment, ChemEngineering 7 (2023). https://doi.org/10.3390/chemengineering7060104.

[14] I. Kanungo, N.N. Fathima, J.R. Rao, B.U. Nair, Influence of PCL on the material properties of collagen based biocomposites and in vitro evaluation of drug release, Mater. Sci. Eng. C 33 (2013) 4651–4659. https://doi.org/10.1016/J.MSEC.2013.07.020.

[15] G. El Fawal, H. Hong, X. Mo, H. Wang, Fabrication of scaffold based on gelatin and polycaprolactone (PCL) for wound dressing application, J. Drug Deliv. Sci. Technol. 63 (2021) 102501. https://doi.org/10.1016/J.JDDST.2021.102501.

[16] B. Banimohamad-Shotorbani, A. Rahmani Del Bakhshayesh, A. Mehdipour, S. Jarolmasjed, H. Shafaei, The efficiency of PCL/HAp electrospun nanofibers in bone regeneration: a review, J. Med. Eng. Technol. 45 (2021) 511–531. https://doi.org/10.1080/03091902.2021.1893396.

[17] M. Zikri, A. Zulkifli, S.A. Sharbani, D. Nordin, N. Shaari, & Siti, K. Kamarudin, Synthesis of Polycaprolactone-Hydroxyapatite (PCL-HA) Biodegradable Nanofibres Via an Electrospinning Technique for Tissue Engineering Scaffolds, J. Kejuruter. 33 (2021) 935–941. https://doi.org/10.17576/jkukm-2021-33.

[18] M. CHEN, P.K. PATRA, S.B. WARNER, S. BHOWMICK, Optimization of Electrospinning Process Parameters for Tissue Engineering Scaffolds, Biophys. Rev. Lett. 01 (2006) 153–178. https://doi.org/10.1142/s1793048006000148.

[19] A. Doustgani, E. Vasheghani-Farahani, M. Soleimani, S. Hashemi-Najafabadi, Process optimization of electrospun polycaprolactone and nanohydroxyapatite composite nanofibers using response surface methodology, J. Nanosci. Nanotechnol. 13 (2013) 4708–4714. https://doi.org/10.1166/jnn.2013.7188.

[20] K.A.G. Katsogiannis, G.T. Vladisavljević, S. Georgiadou, Porous electrospun polycaprolactone fibers: Effect of process parameters, J. Polym. Sci. Part B Polym. Phys. 54 (2016) 1878–1888. https://doi.org/10.1002/polb.24090.

[21] A. Anindyajati, P. Boughton, A.J. Ruys, Modelling and optimization of polycaprolactone ultrafine-fibres electrospinning process using response surface methodology, Materials (Basel). 11 (2018). https://doi.org/10.3390/ma11030441.

[22] A. Anindyajati, P. Boughton, A.J. Ruys, Study on Processing Parameters of Polycaprolactone Electrospinning for Fibrous Scaffold using Factorial Design, Regen. Eng. Transl. Med. 8 (2022) 321–333. https://doi.org/10.1007/s40883-021-00228-9.

[23] C. Zhang, Y. Li, P. Wang, H. Zhang, Electrospinning of nanofibers: Potentials and perspectives for active food packaging, Compr. Rev. Food Sci. Food Saf. 19 (2020) 479–502. https://doi.org/10.1111/1541-4337.12536.

[24] L.A. Can-Herrera, A.I. Oliva, M.A.A. Dzul-Cervantes, O.F. Pacheco-Salazar, J.M. Cervantes-Uc, Morphological and mechanical properties of electrospun polycaprolactone scaffolds: Effect of applied voltage, Polymers (Basel). 13 (2021) 1–16. https://doi.org/10.3390/polym13040662.

[25] X. Qin, D. Wu, Effect of different solvents on poly(caprolactone)(PCL) electrospun nonwoven membranes, J. Therm. Anal. Calorim. 107 (2012) 1007–1013. https://doi.org/10.1007/s10973-011-1640-4.

[26] S.N. Gorodzha, M.A. Surmeneva, R.A. Surmenev, Fabrication and characterization of polycaprolactone cross- linked and

highly-aligned 3-D artificial scaffolds for bone tissue regeneration via electrospinning technology, IOP Conf. Ser. Mater. Sci. Eng. 98 (2015). https://doi.org/10.1088/1757-899X/98/1/012024.
[27] E.M. Abdelrazek, A.M. Hezma, A. El-khodary, A.M. Elzayat, Spectroscopic studies and thermal properties of PCL/PMMA biopolymer blend, Egypt. J. Basic Appl. Sci. 3 (2016) 10–15. https://doi.org/10.1016/j.ejbas.2015.06.001.
[28] G. Zhu, L.Y. Zhao, L.T. Zhu, X.Y. Deng, W.L. Chen, Effect of Experimental Parameters on Nanofiber Diameter from Electrospinning with Wire Electrodes, IOP Conf. Ser. Mater. Sci. Eng. 230 (2017). https://doi.org/10.1088/1757-899X/230/1/012043.
[29] V. Pillay, C. Dott, Y.E. Choonara, C. Tyagi, L. Tomar, P. Kumar, L.C. Du Toit, V.M.K. Ndesendo, A review of the effect of processing variables on the fabrication of electrospun nanofibers for drug delivery applications, J. Nanomater. 2013 (2013). https://doi.org/10.1155/2013/789289.
[30] S. Zargham, S. Bazgir, A. Tavakoli, A.S. Rashidi, R. Damerchely, The effect of flow rate on morphology and deposition area of electrospun nylon 6 nanofiber, J. Eng. Fiber. Fabr. 7 (2012) 42–49. https://doi.org/10.1177/155892501200700414.
[31] A. Haider, S. Haider, I.K. Kang, A comprehensive review summarizing the effect of electrospinning parameters and potential applications of nanofibers in biomedical and biotechnology, Arab. J. Chem. 11 (2018) 1165–1188. https://doi.org/10.1016/j.arabjc.2015.11.015.
[32] T. Wang, S. Kumar, Electrospinning of polyacrylonitrile nanofibers, J. Appl. Polym. Sci. 102 (2006) 1023–1029. https://doi.org/10.1002/app.24123.
[33] K.P. Matabola, R.M. Moutloali, The influence of electrospinning parameters on the morphology and diameter of poly(vinyledene fluoride) nanofibers- Effect of sodium chloride, J. Mater. Sci. 48 (2013) 5475–5482. https://doi.org/10.1007/s10853-013-7341-6.